

Omega-Shaped Tag Antenna with Inductively-Coupled Feeding Using U-Shaped Stepped-Impedance Resonators for RFID Applications

Adam R. H. Alhawari¹, A. H. M. Almawgani¹, Hisham Alghamdi¹, Ayman T. Hindi¹,
Tale Saeidi², and Alyani Ismail³

¹Electrical Engineering Department, College of Engineering, Najran University, Najran, Saudi Arabia
aralhawari@nu.edu.sa, ahalmawgani@nu.edu.sa, hg@nu.edu.sa, athindi@nu.edu.sa

²Department of Electrical and Electronics Engineering, Universiti Teknologi Petronas, Tronoh, Perak, Malaysia
gs32772@gmail.com

³Wireless and Photonic Network Research Center, Department of Computer and Communication Systems Engineering,
Faculty of Engineering, Universiti Putra Malaysia, Malaysia
alyani@upm.edu.my

Abstract — This study proposes a new omega-shaped tag antenna with inductively-coupled feeding (ICF) using U-shaped stepped-impedance resonators (SIRs). It aims at improving the performance of the tag antennas for Radio Frequency Identification (RFID) applications. The radiating body of the antenna is fed using two mirroring symmetrical U-shaped SIRs. This antenna is a simpler alternative for the existing antennas that match the impedance of the antenna to the chip impedance effectively applying varied reinforcement of the equivalent inductance of the radiating structure. In addition to the use of an omega-shaped structure, the proposed feeding technique boosts performance of the antenna impedance, dimensions, and peak gain. The measured size of the antenna was $50 \times 55.55 \times 1.6$ mm³. It attains a peak gain of 1.8 dBi and radiation efficiency higher than 85% at its operating frequency. The experimental results revealed that this tag antenna has the characteristic of good impedance matching within the frequency range of 900-940 MHz, corresponding to a better power reflection coefficient of -3 dB. Comparison between the measured and simulated results verified that the proposed feeding method is capable to improve overall performance of RFID tag antennas.

Index Terms — Inductively-coupled feed, omega-shape, Radio Frequency Identification (RFID), RFID tag, stepped-impedance resonator.

I. INTRODUCTION

The RFID technology is swiftly progressing to produce simpler and more efficient object identification. Currently, it is inevitable to avoid the rapidly-growing applications of RFID in daily life, particularly passive RFID applications. For example, RFID antennas and

sensors are not only embedded into general detection systems, but also involved modern vehicle and transportation devices, access point networks, business transactions, healthcare purposes, and logistics systems [1], [2].

Essentially, the ideal passive RFID tag relies on agreeably matching an antenna into a chip tag, which is combined in a circuit. The perfect matching enhances the chip functionality power, hence, extending the reading range. The most vital section of each passive RFID is considered as the tag antenna. There is growing interest in reducing the cost and size of the RFID for varied applications in numerous fields especially where cost of fabrication and matching networks concerned. The only way is to achieve a direct matching between the antenna and the chip. The suggested approach is to solve the complicated impedance problem, albeit, its variable factors, frequency and the input power magnitude [3].

Recently, among the solutions applied are these tag antennas for RFID purposes mentioned in [4]–[10]. Regrettably, only a few of them offered high omnidirectional gain antennas with miniaturized dimensions. Thus, the urgency is concentrated more on designing methods. For example, an inspiring low-profile antenna design was proposed in [4] that employed a “Vivaldi-like” aperture loaded with meander line and then fed through a slot line which was electromagnetically coupled with the microstrip line. This antenna utilized an ordinary 50-Ω impedance system instead of common chip impedance at a -2.97 dB peak gain. Meanwhile, in [5], a proposed dual-band tag antenna was functioning at both HF and UHF bands. It comprised a spiral shape coil and two meander lines to resonate at HF and UHF bands, respectively. Moreover, it could be easily adjusted and the antenna using various means to handle the coarse and

fine-tuning. Despite these benefits, it is still considered large at the dimensions of $51.4 \times 83.6 \text{ mm}^2$ with a maximum gain of almost -1.5 dB . Another research by Tang et al. [6] developed a rectangular-loop feeding antenna with a bent meandered strip and extra patches to allow it to function in the UHF RFID bands. However, the size of this proposed antenna is $77.5 \times 22.2 \text{ mm}^2$ at maximal gain: 1.6 dB .

Several RFID tag antennas were developed with some configurations specifically optimized to be mountable on metallic objects [11]–[14]. Those RFID tag antennas performance offered low gain because of their reduced size. Other different designs of RFID antennas were proposed in [15]–[18] with inductively-coupled feeding (ICF) designed to improve the gain of tag antennas. This proposed feeding method, specifically ICF, yields enhanced performance in relation to gain and impedance. However, the sizes of the antennas presented in [15]–[18] were still considered big. Therefore, the size required further reduction.

A unique broadband UHF RFID tag antenna for bio-monitoring applications was proposed in [19]. This antenna has a bandwidth of 120 MHz , which allows it to operate at all the UHF frequency band. The levels of performance were improved in both free space and on the human body. Yet, at approximately $80 \text{ mm} \times 50 \text{ mm} \times 200 \text{ }\mu\text{m}$, the size of this antenna is still big. Another RFID tag was designed to detect the dielectric materials in [20]. The basic configuration of this antenna included a printed spiral configuration. The testing results confirmed it could produce tags with acceptable readability and showed a reading distance of up to 7 m when incorporated with metallic objects and 10 m in the case of dielectric objects. But it is also big at $115 \times 26 \times 3.38 \text{ mm}^3$. Next in the list is a high-performance UHF RFID tag antenna consisting of a liquid-filled bottle [21]. It comprised of a folded dipole and a loop-matching unit placed on a water bottle. The testing results determined that the reading range of this antenna can reach up to 4.2 m when placed on a water bottle at the frequency of 915 MHz . Ironically, without the bottle, the reading range of this antenna increased significantly and reached up to 8 m . Yet, it remains a challenge to design a high-performance RFID tag antenna that is suitable to be placed onto a liquid-filled bottle due to the variety of potential liquids and the associated high conductivities and permittivity.

After further review of the literature, this study set forth with the objective to design a cost-effective, high gain, and miniaturized tag antenna with minimal losses to use in RFID applications. The proposed design is based on ICF using U-shaped SIRs that are tuned to operate at a center frequency of 0.915 GHz . Section 2 presents a detailed analysis of the suggested stepped-impedance resonator feeding. Then, the configuration of the proposed tag antenna follows in Section 3. Both the

theoretical and evaluated results are presented in Section 4 and then it is concluded in Section 5.

II. ANALYSIS OF THE FEED STRUCTURE OF THE U-SHAPED STEPPED-IMPEDANCE RESONATOR

The stepped-impedance resonators (SIRs) are used extensively in the designs of microstrip and microwave devices for their easier regulator and miniature size. Exclusively, previous studies reported in [22]–[24] reported that the SIRs are tunable over a wide range of frequencies by the effect of the impedance ratio (R_z) of the low-impedance to the high-impedance sections. Once R_z is reduced, the resonator length will also be minimized. The flexibility in reducing the length of the resonator is beneficial in meeting the miniaturization demand of the industry.

Figure 1 shows the U-shaped SIR feeding configuration. It is fed based on two symmetrical U-shaped SIR units to excite the radiating dipole via ICF. Its opposite central points directly connected to the RFID chip at the head of the two U-shaped SIR structures (Fig. 1). The equivalent inductance in the previously stated dipole is achieved by utilizing the proposed feeding configuration. The parameters S_U , L_{Z1} , L_{Z2} , W_{Z1} and W_{Z2} provide flexible control over the inductive coupling strength. Figure 2 depicts the ICF's equivalent circuit. The inductive-coupling unit can be turned into a transformer. The Z_{in} known as the antenna input impedance, is recorded at the terminals of the U-shaped SIR and is estimated as follows [15]:

$$Z_{in} = R_{in} + jX_{in} = \frac{(2\pi f M)^2}{Z_{ant}} + Z_U, \quad (1)$$

where Z_{ant} and Z_U are the dipole antenna impedance and the U-shaped SIR feeds impedance, respectively. Likewise, M has shared inductance between the two impedances. The value of Z_U can be calculated using Equation 2:

$$Z_U = j2\pi f L_U, \quad (2)$$

where L_U is the self-inductance of the SIR feed structure. The equation 3 can assist to calculate the antenna impedance at the resonant frequency ($f = f_0$) of dipole antenna as:

$$Z_{in} = \left(\frac{(2\pi f_0 M)^2}{Z_{ant}} \right) + (j2\pi f_0 L_U). \quad (3)$$

Equation 3 confirms that the inductance of the U-shaped SIR (L_U) specifies the input reactance. Meanwhile, the transformer mutual inductance (M) determines the resistance regardless of whether the radiating dipole antenna is operating at the resonance frequency or at any other frequencies. Theoretically, reactance and resistance can be adjusted independently. Besides, the proposed feeding structure is a simple and ideal alternative to match the antenna impedance to the chip impedance effectively.

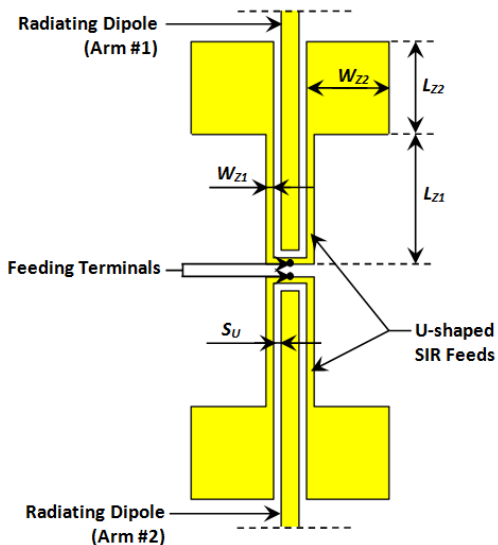


Fig. 1. The proposed layout of ICF using the U-shaped SIRs.

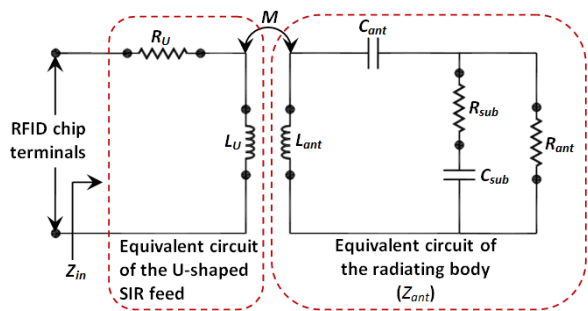


Fig. 2. The equivalent circuit model of ICF.

Figures 3, 4, 5, 6, and 7 shows plots, indicating how the U-shaped SIR designing parameters such as L_{Z1} , L_{Z2} , W_{Z1} , W_{Z2} , and S_U affecting the return loss (dB) results. The return loss plots were simulated using Murata RFID MAGICSTRAP LXMS31ACNA-011 tag chip, with input impedance of $(25-j200) \Omega$ at resonance frequency of 915 MHz. The simulation results summary is any increment in the L_{Z1} will reduce the resonant frequency. In contrary, it works for different values of the impedance ratio (R_Z). The results demonstrate that any increment in R_Z value will affect the resonant frequency of the tag antenna and shift it down. It can be concluded that R_Z is a vital electrical parameter for characterizing properties of the U-shaped SIRs feeding structure. Therefore, the selection of R_Z offers a flexible method to tune the resonant frequency of the tag antenna to the desired operating frequency.

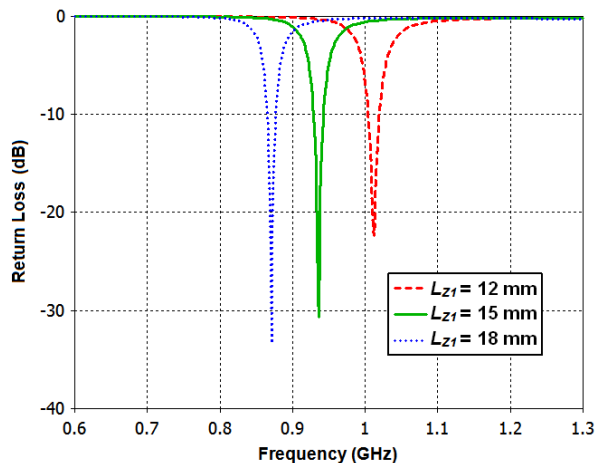


Fig. 3. Simulated return loss at different L_{Z1} values.

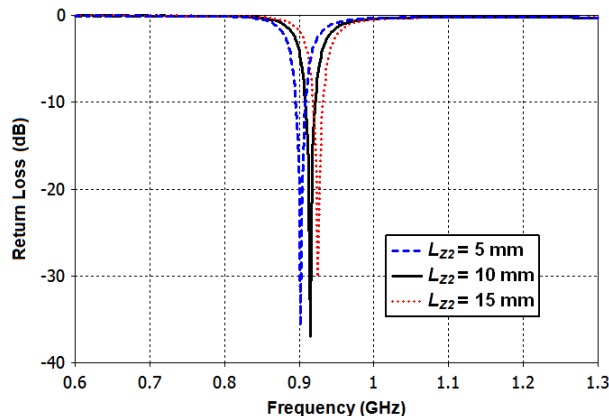


Fig. 4. Simulated return loss at different L_{Z2} values.

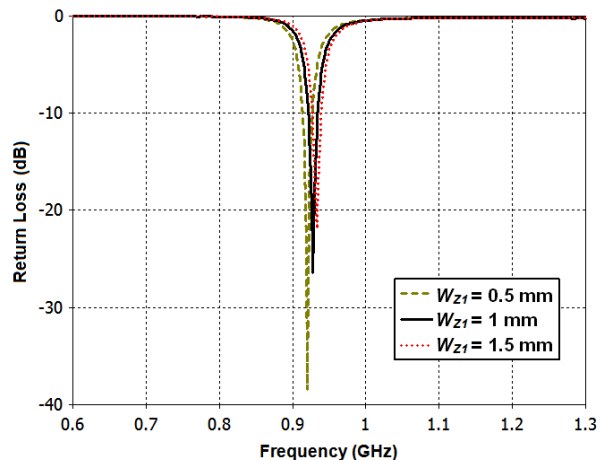


Fig. 5. Simulated return loss at different W_{Z1} values.

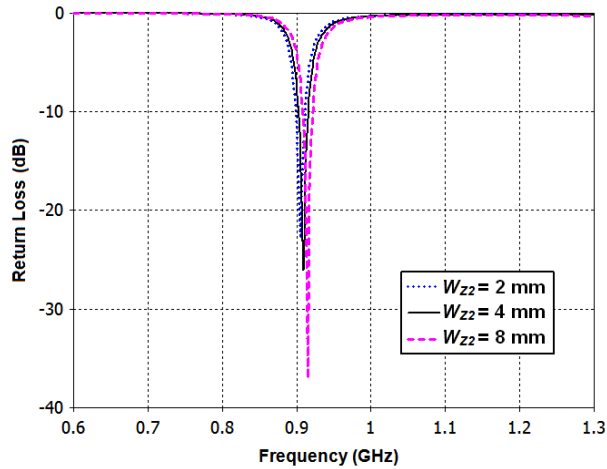


Fig. 6. Simulated return loss at different W_{z2} values.

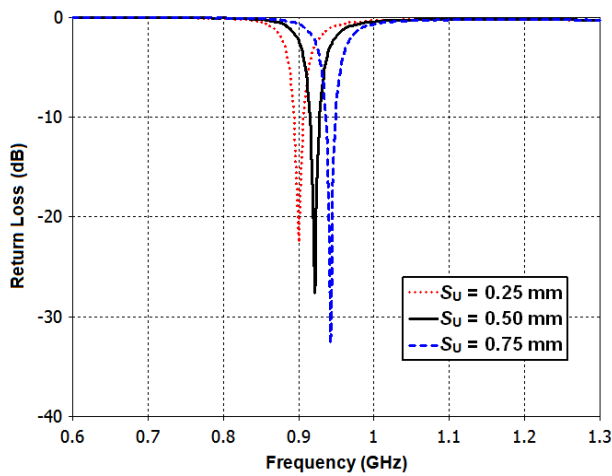


Fig. 7. Simulated return loss at different S_U values.

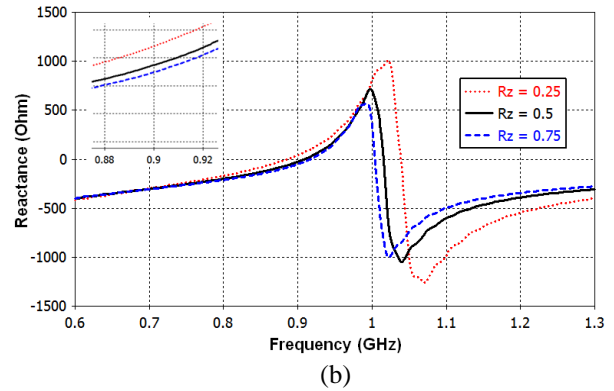
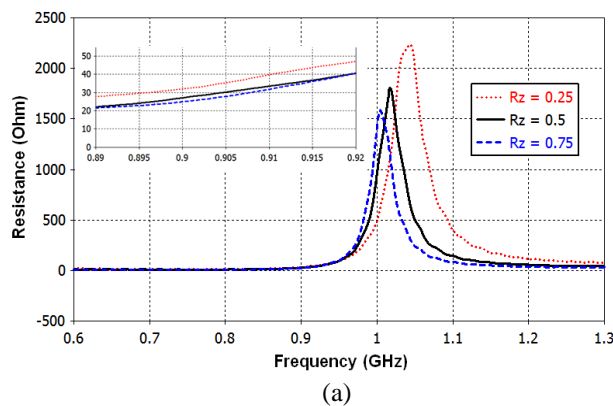


Fig. 8. Simulated input impedance of the tag antenna for different values of R_z : (a) resistance and (b) reactance.

III. CONFIGURATION OF THE PROPOSED TAG ANTENNA

A miniaturized microstrip tag antenna is proposed for RFID purposes. It comprises of two U-shaped ICF SIR arms and an omega-shaped resonator as a radiating dipole body. The omega-shaped resonator configurations have competent resonance property and can shrink the length of the resonator, in which such adjustment is frequently adapted by the researchers in many designs applications to meet higher performance enhancement and miniaturization targeted like in the reported works in [25]–[28]. However, based on the authors' knowledge, it has been used solely in the development of RFID tag antennas as proposed in this work.

In this antenna design procedure, both structures (the U-shaped ICF SIR arms and the omega-shaped radiating dipole body) are located on the upper surface of the substrate (Fig. 9). Also, it has no conductor attached to the bottom surface of the substrate. The absence of any direct contact material is purposely done to avoid obstruction during experimental sessions. Its elliptical shapes, and dimensions were carefully specified to improve impedance matching. Its IC chip terminals are placed directly in the middle of the two opposing U-shaped SIR units. Encouragingly, the mutual coupling assists the feeding to communicate with the body of the tag antenna. That is how it offers attractive features in sensing applications. Figures 9 and 10 show the simulated and fabricated prototype of the proposed RFID tag antenna, respectively. Additionally, the geometrical properties of this antenna are tabulated in Table 1. The values of the listed geometrical properties are the optimized values for better functionality to obtain the

antenna in its UHF operation frequency RFID band from 860 to 960 MHz. These optimized values (Table 1) were gained during the simulation process.

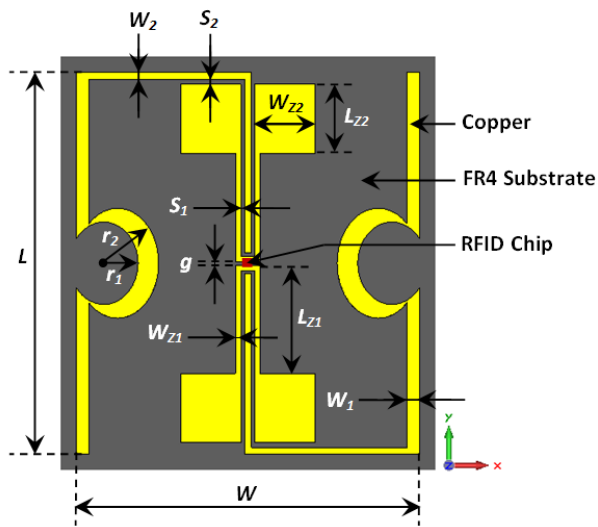


Fig. 9. The simulated prototype of the proposed tag antenna.

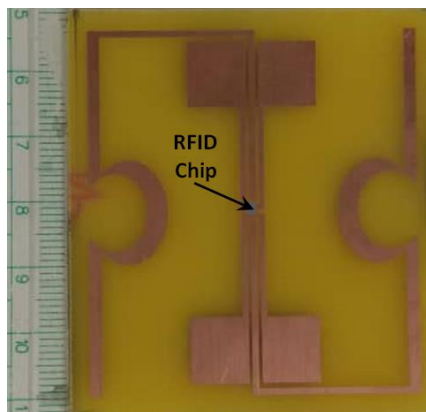


Fig. 10. The fabricated tag antenna prototype.

A Murata RFID MAGICSTRAP LXMS31ACNA-011 tag chip [29] was utilized to fabricate the antenna. At assumed $(25-j200) \Omega$ input impedance and operating at 915 MHz resonant frequency, the minimum point of threshold power is -8 dBm. This tag antenna was fabricated on an epoxy FR4 substrate with a loss tangent of 0.02, $h = 1.6$ mm, and $\epsilon_r = 4.4$. Its measurement is $50 \times 55.55 \times 1.6$ mm³. These dimensions, as well as the resonance frequency of this antenna, are based on optimized simulations that matched the inductance with a conjugate impedance of the selected chip. Furthermore, it has miniaturized dimensions corresponding reductions of nearly 20.64%, 30.5%, 7.1%, 32.18%, and 22.84% in size compared to those antennas proposed in [16], [19], [20], [30], [31], respectively.

The CST Microwave Studio 2019 was used as a full-wave electromagnetic simulator to simulate the proposed tag antennas characteristics using Finite-Difference Time-Domain (FDTD) method [32]. Figures 11 and 12 depict the simulated return losses (R_L) of the proposed antenna in terms of W_1 and W_2 , respectively. This step was taken to determine what influences the width of the omega-shaped antenna from its overall performance. The values of parameters presented in Table 1 are considered in the simulation process. It suggests that the increases in W_1 and W_2 will slightly increase the frequency response of the antenna. Therefore, it is concluded that the dimensions of the omega-shaped antenna largely influence its performance.

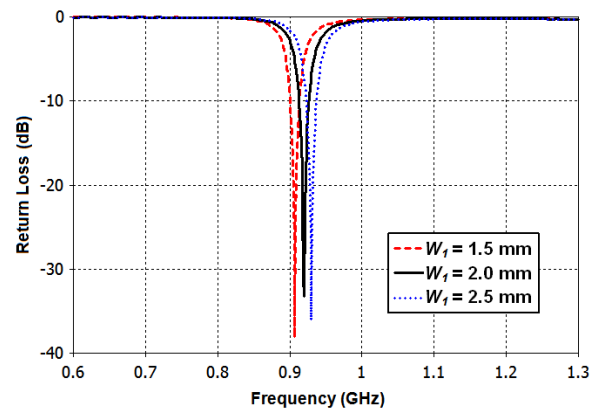


Fig. 11. The simulated return loss of the proposed antenna in terms of W_1 .

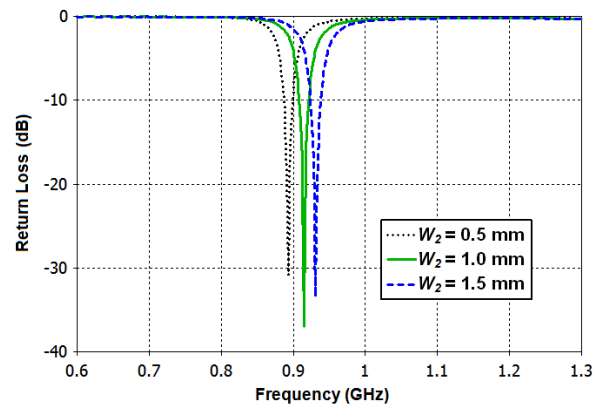


Fig. 12. The simulated return loss of the proposed antenna in terms of W_2 .

Figure 13 indicates a plot of the simulated R_L of tag for three antennas of different geometrical shapes according to the geometrical parameters of the antenna listed in Table 1. The simulation results shown in the figure were intended to compare the properties and performance among antenna designs: the proposed design, the ones without omega-shape and without the

U-shaped SIRs. The results (Fig. 13) demonstrate that the proposed tag antenna yields better results in terms of R_L , lower than -35 dB compared to other antennas configurations. Therefore, by combining both techniques of design structures (the U-shaped SIR resonator as feeder structure and the Omega-shaped as a radiating body of the antenna) simultaneously overcomes the mismatching problem between the antenna and its chip impedances. Consequently, also solves the antenna size problems. In fact, using the U-shaped SIR resonator as a feeder structure offers an easier controlling method for resonant frequency by adjusting the impedance ratio (the low-impedance to the high-impedance). However, there are rooms to improve better matching techniques between the antenna impedance and the IC chip impedance. Additionally, the omega-shaped insertion turns the resonator length of the dipole antenna shrinkable. The reducible length of the resonator is advantageous in meeting the miniaturization demand of the industry. Overall, researchers found that the proposed design for the tag antenna meets the current engineering demands on the antenna design for RFID applications.

Next, the lumped-element values of the equivalent circuit model of the proposed ICF tag antenna shown in Fig. 2 were optimized using CST design studio modelling, including its material substrate effects. Then, the results were compared with the ones obtained from the 3D full-wave model as illustrated in Fig. 14. The simulated return loss of the tag antenna shown in Fig. 14 were simulated by considering the lumped-element values of chip impedance operating at the frequency of 915 MHz (based on the geometrical parameters in Table 1). Obviously, both the modeled and the full wave simulated results seemed in good agreement, which validates the equivalent circuitual model illustrated in Fig. 2. Also, Fig.

14 indicates that the antenna performs well in terms of the achieved return loss, which is lower than -30 dB.

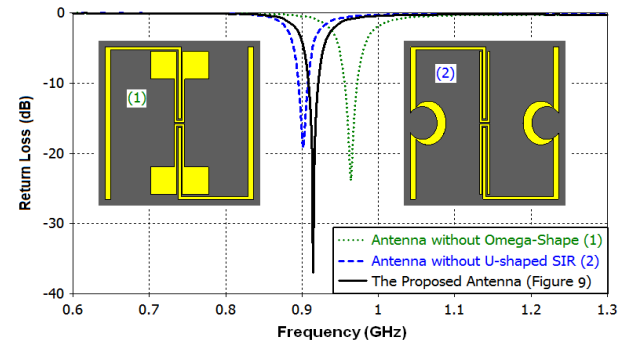


Fig. 13. The simulated return loss results for three various geometrical shapes.

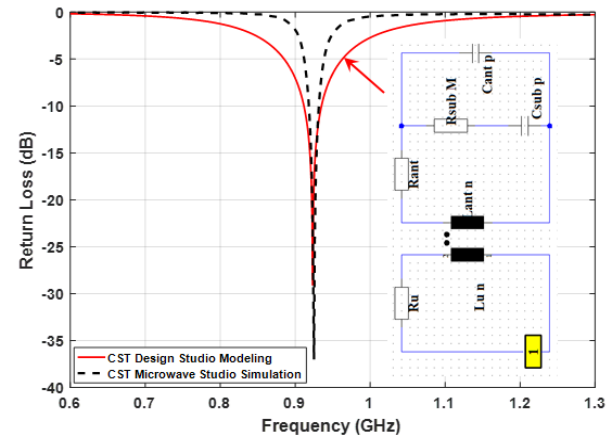


Fig. 14. Comparison between modeled data and full wave simulated results.

Table 1: The antenna designing parameters

Parameter	L	W	W_1	W_2	S_1	S_2	L_{Z1}	L_{Z2}	W_{Z1}	W_{Z2}	r_1	r_2	g
Value (mm)	55.55	50	1.8	1.0	0.5	0.75	15.78	10	0.8	8	5	8	0.5

IV. EXPERIMENTAL RESULTS AND DISCUSSION

In order to conduct standard measurement, a differential probe was utilized in a room environment. The differential probe has a symmetrical structure and it was originally developed by Palmer et al. [33]. Two ports are connected through a fixture with the metal shields of the semi-rigid coaxial cables soldered to build the virtual common ground. After that, the free space measurement was administered connecting the differential probe to a Vector Network Analyzer (Anritsu 37347D model) at one end and then it is soldered to the tag antenna from the other end.

Figure 15 illustrates the comparison between the measured and the simulated impedance results. The

former results were achieved after de-embedding the effect of the semi-rigid cables from the reflection and transmission coefficients. And then it was measured at the Sub-Miniature Version A (SMA) connectors applying the technique presented in [33], [34]. Figure 15 shows only a slight difference in the resistance and reactance curves in both measured and simulated results. The main difference observed between these values (Fig. 15) can be attributed to the soldered measurement probe. Another potential explanation is any probable mismatch between the SMA connectors and feeding lines, the potential defects in the fabrication process, and the variations of chip impedance, are usually common in the real implementation. Additionally, Fig. 15 uncovers that the measured and simulated impedances at the center

frequency of 915 MHz are $(12.98 + j191.7) \Omega$ and $(24.77 + j200.2) \Omega$, respectively.

In other respects, the present study followed the method for the power reflection coefficient (PRC) analysis described in [35]. The simulated and measured PRC results of the proposed tag antenna with half-power bandwidth (HPBW) are shown in Fig. 16. The HPBW is defined based on the $\text{PRC} < -3$ dB criterion. The simulated and measured HPBW values are 1.97% (906-924 MHz) and 4.35% (900-940 MHz), respectively (their center frequencies are 915 MHz and 919 MHz). The measured results are varied slightly from the simulated results and it might be due to many main reasons such as fabrication process defects, a variation of the chip impedance as well as the soldering imperfection that exists between the differential probe and the tag antenna. In addition, the measurement carried out in a normal room environment, not inside an anechoic chamber. Nonetheless, the results prove that the antenna is working within the standard UHF frequency RFID band between 860 and 960 MHz.

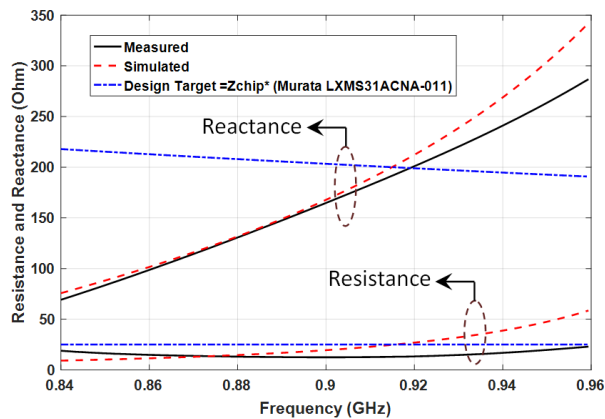


Fig. 15. The measured and simulated impedance.

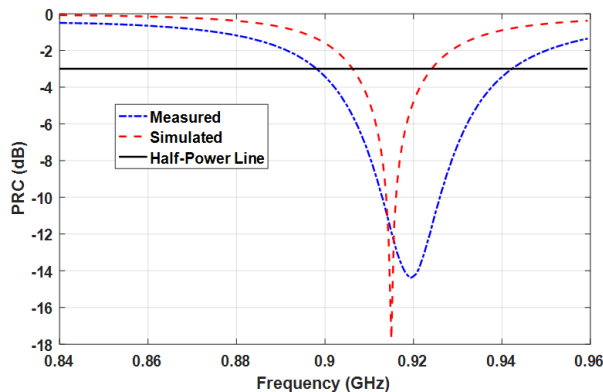


Fig. 16. The power reflection coefficient values in measurement and simulation.

The maximum possible theoretical read range (r_{\max}) of the proposed tag antenna can be computed using Friis free-space method [3]:

$$r_{\max} = \frac{\lambda}{4\pi} \sqrt{\frac{P_t G_t G_r}{P_{th}}}, \quad (4)$$

where λ is the wavelength, P_t represents the power transmitted by the reader, G_t is the gain of the reader antenna, G_r is the gain of the receiving tag antenna, and P_{th} is the minimum threshold power that required to turn on the chip.

The highest theoretical reading range of the proposed tag antenna calculated using Equation 4 was 5.56 m. To verify the match of the actual reading range with this theoretical value, the measurements were performed at a setting of 30 dBm output power for the reader corresponded to a nearly 4.0 W of equivalent isotropic radiated power (EIRP). With the ATid (AT-870) hand-held reader, the reading range measured 5.1 m, which is approximately 8.2% lower than the maximum theoretical reading range. This difference between the calculated (theoretical) and measured (actual) reading ranges has mainly ascribed the fact that the measurements were taken in the normal room environment.

Figure 17 demonstrates the simulated and measured peak gain of the proposed antenna at the desired UHF RFID frequency band. For further investigation, the simulated radiation efficiency and the far-field radiation pattern of the proposed tag antenna are presented in Figs. 18 and 19, respectively. Besides, the proposed antenna achieves an omnidirectional gain of 1.8 dBi and radiation efficiency of almost 85% at 0.915 GHz which are higher than those presented in [4]–[6], [11], [13], [14], [18]–[20], [30], [36]. The main improvement of this antenna compared to previous ones is its enhanced performance by ICF using the U-shaped SIRs and the omega shaped design. These parts add inductance to the radiating dipole antenna that does not exist in the conventional feeding techniques such as the coupled open-loop reported in [15].

In order to verify further and highlight the originality of the proposed tag antenna design and feeding configuration, a comparison was made with several recently developed UHF RFID tag antennas in terms of antenna dimensions, gain, and the reading range. The comparisons (Table 2) reveal that the propose one presents size reduction of 20.64%, 30.5%, 7.1%, 32.18%, and 22.84% as compared to the antennas reported in [16], [19], [20], [30], [31], [36], respectively. Furthermore, a higher peak gain is obtained in comparison with tag antennas introduced in [14], [19]–[21], [30], [31], [36] at 915 MHz. Moreover, the proposed antenna shows a longer read range as compared to similar

works in [14], [16], [19], with a better improvement for radiation efficiency. However, the proposed antenna uses the same value of chip impedance ($25-j200 \Omega$) with the antennas reported in [14], [16]. The proposed antenna features a lower read range compared to some existing RFID antennas reported in [20], [21], [30] because of the high minimum threshold power required to turn on the MURATA chip of -8 dBm ($160 \mu\text{W}$). Using another type of chip may improve the effectiveness in extending the read range further. For instance, some of them may offer lower minimum threshold power (e.g., NXP Ucode8 chip with threshold sensitivity of -20 dBm). Accordingly, the proposed design attracts RFID applications that demand economical choice of compact-sized antennas, an extended reading range, and good performance concerning the gain and radiation efficiency.

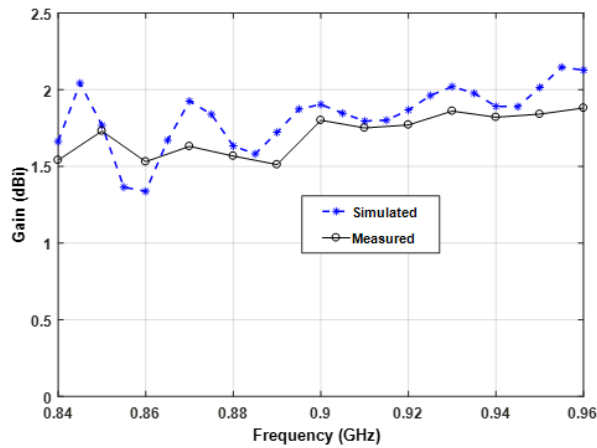


Fig. 17. The measured and simulated realized gain.

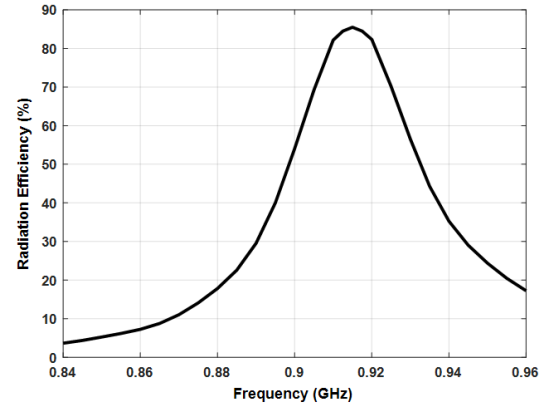


Fig. 18. Simulated antenna radiation efficiency.

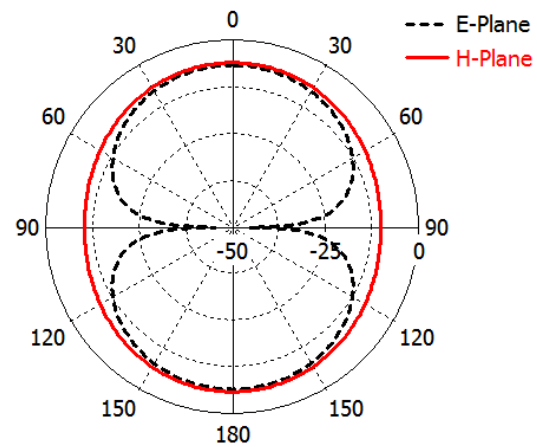


Fig. 19. Simulated far-field radiation pattern at the frequency of 915 MHz.

Table 2: Comparison between the proposed RFID tag antenna and recently developed works

Reference	Chip Impedance (Ω) at 915 MHz	Size (mm^2)	Gain (dBi)	Reading Range (m)
[14]	$25-j200$	82.75×19.5	-0.53	3.72
[16]	$25-j200$	50×70	2.50	4.92
[19]	$23-j202$	80×50	1.75	4.6
[20]	$25-j237$	115×26	2.08	7.5
[21]	$24.5-j190$	44×20	-5.54	5.6
[30]	-	64×64	-1.18	10.2
[31]	$13.5-j111$	60.1×60.1	0.25	6.7
[36]	$13.5-j111$	60×60	-9.7	3.36
Proposed Antenna	$25-j200$	50×55.55	1.80	5.1

VI. CONCLUSION

This study develops an omega-shaped tag antenna with ICF using U-shaped SIRs for RFID applications. It consists of two omega-shaped radiating arms that are fed by an innovative method implementing ICF using U-shaped SIRs to reduce the antenna size and improve the gain. It produces an inductance that is equivalent to the radiating dipole antenna. Hence, it offers a transformative

method to augment the strength of inductive coupling as well as a simple alternative to perfectly match between antenna and impedance. Furthermore, the simulated and measured results present an omnidirectional peak gain of nearly 1.8 dBi. This peak gain (1.8 dBi) is higher than the peak gains of the traditional antennas recently proposed in [14], [19]–[21], [30], [36]. In addition, the herein proposed tag antenna has a compact size with an

area of just $50 \times 55.55 \text{ mm}^2$. As such, it is 20.64%, 30.5%, 7.1%, 32.18%, and 22.84% smaller in size than the tag antennas proposed recently in [16], [19], [20], [30], [31], respectively. It can be concluded that the tag antenna proposed in this paper has a better overall performance than the other tag antennas due to its higher radiation efficiency, size, gain, and impedance. The overall results of this study suggests turning it into a more desirable design for its potentialities for various applications of the UHF RFID systems.

ACKNOWLEDGMENT

The authors would like to express their gratitude to the Ministry of Education and the Deanship of Scientific Research – Najran University – Kingdom of Saudi Arabia for their financial and technical support under code number (NU/ESCI/16/015).

REFERENCES

- [1] H. Li and Y. Ren, "Design and implementation of building structure monitoring system based on radio frequency identification (RFID)," *International Journal of RF Technologies*, vol. 9, pp. 37-49, Aug. 2018.
- [2] R.-S. Hsiao, C.-H. Kao, T.-X. Chen, and J.-L. Chen, "A passive RFID-based location system for personnel and asset monitoring," *Technology and Health Care*, vol. 26, pp. 1-6, Oct. 2017.
- [3] K. V. S. Rao, P. V. Nikitin, and S. F. Lam, "Antenna design for UHF RFID tags: A review and a practical application," *IEEE Transactions on Antennas and Propagation*, vol. 53, no. 12, pp. 3870-3876, 2005.
- [4] E. A. Soliman, M. O. Sallam, W. De Raedt, and G. A. E. Vandenbosch, "Miniaturized RFID tag antenna operating at 915 MHz," *IEEE Antennas and Wireless Propagation Letters*, vol. 11, pp. 1068-1071, 2012.
- [5] Z. L. Ma, L. J. Jiang, J. Xi, and T. T. Ye, "A single-layer compact HF-UHF dual-band RFID tag antenna," *IEEE Antennas and Wireless Propagation Letters*, vol. 11, pp. 1257-1260, 2012.
- [6] Z.-J. Tang, J. Zhan, Z.-F. Xi, and Y.-G. He, "Broadband UHF RFID tag antenna with a rectangular-loop feed and additional patches," *Microwave And Optical Technology Letters*, vol. 54, no. 5, pp. 1234-1236, 2012.
- [7] A. A. Babar, S. Manzari, L. Sydanheimo, A. Z. Elsherbeni, and L. Ukkonen, "Passive UHF RFID tag for heat sensing applications," *IEEE Transactions on Antennas and Propagation*, vol. 60, no. 9, pp. 4056-4064, 2012.
- [8] X. Chen, L. Ukkonen, and T. Björninen, "Passive E-textile UHF RFID-based wireless strain sensors with integrated references," *IEEE Sensors Journal*, vol. 16, no. 22, pp. 7835-7836, 2016.
- [9] P. Escobedo, M. A. Carvajal, L. F. Capitán-Vallvey, J. Fernández-Salmerón, A. Martínez-Olmos, and A. J. Palma, "Passive UHF RFID tag for multispectral assessment," *Sensors (Switzerland)*, vol. 16, no. 7, 2016.
- [10] C. K. Stoumpos, D. E. Anagnostou, and M. T. Chryssomallis, "Experimental characterization of the impedance of balanced UHF RFID tag antennas," *Microwave and Optical Technology Letters*, vol. 59, no. 12, pp. 3127-3134, Dec. 2017.
- [11] P. Yang, S. He, Y. Li, and L. Jiang, "Low-profile microstrip antenna with bandwidth enhancement for radio frequency identification applications," *Electromagnetics*, vol. 32, no. 4, pp. 244-253, 2012.
- [12] T. Deleruyelle, P. Pannier, M. Egels, and E. Bergeret, "An RFID tag antenna tolerant to mounting on materials," *IEEE Antennas and Propagation Magazine*, vol. 52, no. 4, pp. 14-19, 2010.
- [13] A. S. A. Jalal, A. Ismail, A. R. H. Alhawari, M. F. A. Rasid, N. K. Noordin, and M. A. Mahdi, "Miniaturized metal mount Minkowski fractal RFID tag antenna with complementary split ring resonator," *Progress In Electromagnetics Research C*, vol. 39, no. Apr., pp. 25-36, 2013.
- [14] F. Erman, E. Hanafi, E.-H. Lim, W. A. W. M. Mahyiddin, S. W. Harun, H. Umair, R. Soboh, and M. Z. H. Makmud, "Miniature compact folded dipole for metal mountable UHF RFID tag antenna," *Electronics*, vol. 8, no. 6, p. 713, 2019.
- [15] H.-W. Son and C.-S. Pyo, "Design of RFID tag antennas using an inductively coupled feed," *Electronics Letters*, vol. 41, no. 18, pp. 1-2, 2005.
- [16] A. R. H. Alhawari, A. Ismail, A. S. A. Jalal, R. S. A. R. Abudullah, and M. F. A. Rasid, "U-shaped inductively coupled feed radio frequency identification tag antennas for gain enhancement," *Electromagnetics*, vol. 34, no. 6, 2014.
- [17] M. S. R. Bashri, M. I. Ibrahimy, and S. M. A. Motakabber, "Design of a wideband inductively coupled loop feed patch antenna for UHF RFID tag," *Radioengineering*, vol. 24, no. 1, pp. 38-44, 2015.
- [18] L. Mo and C. Li, "Double loop inductive feed patch antenna design for antimetal UHF RFID tag," *International Journal of Antennas and Propagation*, vol. 2019, 2019.
- [19] D. Marques, M. Egels, and P. Pannier, "Broadband UHF RFID tag antenna for bio-monitoring," *Progress In Electromagnetics Research B*, vol. 67, no. 1, pp. 31-44, 2016.
- [20] K. Siakavara, S. Goudos, A. Theopoulos, and J. Sahalos, "Passive UHF RFID tags with specific printed antennas for dielectric and metallic objects applications," *Radioengineering*, vol. 26, no. 3, pp.

- 735-745, 2017.
- [21] S. He, Y. Zhang, L. Li, Y. Lu, Y. Zhang, and H. Liu, "High performance UHF RFID tag antennas on liquid-filled bottles," *Progress In Electromagnetics Research*, vol. 165, no. July, pp. 83-92, 2019.
- [22] Q.-X. Chu and F.-C. Chen, "A novel dual-band bandpass filter using stepped impedance resonators with transmission zeros," *Microwave and Optical Technology Letters*, vol. 50, no. 6, pp. 1466-1468, Jun. 2008.
- [23] Q.-X. Chu and F.-C. Chen, "A compact dual-band bandpass filter using meandering stepped impedance resonators," *Microwave and Wireless Components Letters, IEEE*, vol. 18, pp. 320-322, Jun. 2008.
- [24] M. Makimoto and S. Yamashita, *Microwave Resonators and Filters For Wireless Communication: Theory, Design and Application*. Berlin: Springer-Verlag, Berlin, Heidelberg, 2001.
- [25] O. Altıntaş, M. Aksoy, and E. Ünal, "Design of a metamaterial inspired omega shaped resonator based sensor for industrial implementations," *Physica E: Low-dimensional Systems and Nanostructures*, vol. 116, no. Aug. 2019, p. 113734, 2020.
- [26] H. Hatefi Ardakani, S. Fallahzadeh, and J. Rashed-Mohassel, "Phase velocities equalization of coupled microstrip lines using Ω -shaped particles and suppression of the second harmonic," *IEEE Transactions on Microwave Theory and Techniques*, vol. 60, no. 3 PART 1, pp. 464-470, 2012.
- [27] M. Labidi, R. Salhi, and F. Choubani, "A design of metamaterial multi-band bowtie antenna based on omega-shaped resonator," *Applied Physics A: Materials Science and Processing*, vol. 123, no. 5, pp. 1-6, 2017.
- [28] K. Aydin, Z. Li, M. Hudlička, S. A. Tretyakov, and E. Ozbay, "Transmission characteristics of bianisotropic metamaterials based on omega shaped metallic inclusions," *New Journal of Physics*, vol. 9, 2007.
- [29] "Murata." [Online]. Available: <https://www.murata.com/products/rfid> [Accessed: 08-Oct-2019].
- [30] E. Yang and H. Son, "Dual-polarised metal-mountable UHF RFID tag antenna for polarisation diversity," *Electronics Letters*, vol. 52, no. 7, pp. 496-498, 2016.
- [31] M. H. Zolghadri and S. Jam, "A wideband circular polarization antenna for UHF tags," *Applied Computational Electromagnetics Society Journal*, vol. 33, no. 3, pp. 319-324, 2018.
- [32] "Computer Simulation Technology (CST) Microwave Studio," 2019.
- [33] K. D. Palmer and M. W. van Rooyen, "Simple broadband measurements of balanced loads using a network analyzer," *IEEE Transactions on Instrumentation and Measurement*, vol. 55, no. 1, pp. 266-272, 2006.
- [34] S. K. Kuo, S. L. Chen, and C. T. Lin, "An accurate method for impedance measurement of RFID tag antenna," *Progress in Electromagnetics Research*, vol. PIER 83, pp. 93-106, 2008.
- [35] P. V. Nikitin, K. V. S. Rao, S. F. Lam, V. Pillai, R. Martinez, and H. Heinrich, "Power reflection coefficient analysis for complex impedances in RFID tag design," *IEEE Transactions on Microwave Theory and Techniques*, vol. 53, no. 9, pp. 2721-2725, 2005.
- [36] U. H. Khan, B. Aslam, J. Khan, M. Nadeem, H. Shahid, M. A. Azam, Y. Amin, and H. Tenhunen, "A novel asterisk-shaped circularly polarized RFID tag for on-metal applications," *Applied Computational Electromagnetics Society Journal*, vol. 31, no. 9, pp. 1035-1042, 2016.



Adam R. H. Alhawari was born in Irbid, Jordan. In 2003, he was awarded a B.Sc. degree in Communication Engineering by Hijawi Faculty for Engineering Technology at Yarmouk University, Jordan. He obtained both postgraduate degree of M.Sc. and Ph.D. degrees in 2009 and 2012, respectively, in Wireless Communications Engineering from Universiti Putra Malaysia. Previously, he started the entry level with the post of Senior Lecturer in Universiti Putra Malaysia from 2012 to 2015. Currently, he was promoted to the Associate Professorship in the Electrical Engineering Department, College of Engineering, Najran University, Saudi Arabia. His main research interests are microstrip filters, metamaterial antennas, and RFID.



A. H. M. Almawgani was born in Ibb, Yemen, in 1979. He received the B.Sc. degree in Information Engineering from the College of Engineering in Baghdad University in 2003. He received the M.Sc. and Ph.D. degrees in Electronic Systems Design Engineering and Communication Engineering from Universiti Sains Malaysia, in 2008 and 2011, respectively. He was an Assistant Professor in the Electrical Engineering Department, Faculty of Engineering, University of Science and Technology, Sana'a, Yemen, until February 2014. Currently, he is an Associate Professor in the Electrical Engineering Department, College of Engineering, Najran

University, Saudi Arabia. His main research interests are signal-processing algorithms with application to telecommunications and wireless communication networks.



Hisham Alghamdi received his M.Sc. degree in Electrical and Electronics Engineering from the University of Leicester, Leicester, UK, in 2010 and his Ph.D. from University of Southampton 2016, respectively. Currently, he is working

as an Assistant Professor in the Electrical Engineering Department at Najran University, Saudi Arabia. His main research areas are in solar energy, building energy technologies and systems, energy efficiency, sustainable and resilient cities, smart grids and energy and environment policies.



Ayman T. Hindi received his B.S. in Electrical Engineering from Vinnitsa Technical University in 1995 and Ph.D. degree in Power Systems Engineering from Vinnitsa Technical University in 2004. Currently he is an Assistant Professor

at the Electrical Engineering Department, Najran University, Saudi Arabia. His main research interests include compensation of reactive power energy and consumption in electric installation and systems.



Tale Saedi was born in Mashhad, Iran in 1985. He received his Bachelor of Science degree in Telecommunication and Electrical Engineering from Khayam University of Mashhad, Iran in 2009 and he completed his Masters in Wireless Communication Engineering from

Universiti Putra Malaysia in 2015. Currently, he is working as a Graduate Assistant in Universiti Teknologi Petronas, Malaysia. His research interest includes dielectric measurement of MW absorber materials, microstrip antenna design for MW, mm-wave and THz frequency bands. Furthermore, metamaterial array UWB antennas in MW and UWB imaging.



Alyani Ismail received her Bachelor of Engineering in Electronic and Information Systems Engineering from the University of Huddersfield, UK. She obtained her M.Sc. in Computer, Communication and Human-Centered Systems from the University of Birmingham, UK

and Ph.D. in Electronics Engineering also from the University of Birmingham. She is currently a Professor at the Department of Computer and Communication Systems Engineering, Faculty of Engineering, Universiti Putra Malaysia (UPM). Alyani's research interests are in the area of Communication Engineering, Wireless Sensors and antenna systems.